

BRIEF REPORT



MeCP2 interacts with chromosomal microRNAs in brain

Abdul Waheed Khan^{a,b,c,*}, Mark Ziemann^{a,b}, Haloom Rafehi^{a,b}, Scott Maxwell^{a,b}, Giuseppe D. Ciccotosto^{c,d} and Assam El-Osta^{a,b,c,e}

^aCentral Clinical School, Faculty of Medicine, Monash University, Victoria, Australia; ^bBaker IDI Heart and Diabetes Institute, The Alfred Medical Research and Education Precinct, Melbourne, Victoria 3004, Australia; ^cDepartment of Pathology, The University of Melbourne, Parkville, Victoria, Australia; ^dBio21 Molecular science and Biotechnology Institute, Victoria, Australia; ^eHong Kong Institute of Diabetes and Obesity, Prince of Wales Hospital, The Chinese University of Hong Kong, Hong Kong SAR

ABSTRACT

Although methyl CpG binding domain protein-2 (MeCP2) is commonly understood to function as a silencing factor at methylated DNA sequences, recent studies also show that MeCP2 can bind unmethylated sequences and coordinate gene activation. MeCP2 displays broad binding patterns throughout the genome, with high expression levels similar to histone H1 in neurons. Despite its significant presence in the brain, only subtle gene expression changes occur in the absence of MeCP2. This may reflect a more complex regulatory mechanism of MeCP2 to complement chromatin binding. Using an RNA immunoprecipitation of native chromatin technique, we identify MeCP2 interacting microRNAs in mouse primary cortical neurons. In addition, comparison with mRNA sequencing data from *Mecp2*-null mice suggests that differentially expressed genes may indeed be targeted by MeCP2-interacting microRNAs. These findings highlight the MeCP2 interaction with microRNAs that may modulate its binding with chromatin and regulate gene expression.

ARTICLE HISTORY

Received 28 June 2017
Revised 28 September 2017
Accepted 8 October 2017

KEYWORDS

MeCP2; microRNAs; RNA-chromatin immunoprecipitation

Introduction

Methyl CpG binding domain protein-2 (MeCP2) is a chromatin-binding factor that was first isolated through its affinity for methylated CpG dinucleotides in 1992.¹ Although ubiquitously expressed, MeCP2 is particularly abundant in neurons and plays a critical role in their development and function. The significance of this role was highlighted in 1999 with the discovery that mutations in the *MECP2* gene resulted in Rett syndrome.² This connection garnered interest in and accelerated MeCP2 research. Rett syndrome, first described by Andreas Rett in 1966, is a postnatal X-linked neurodevelopmental disorder that affects one in 10,000 females.^{3,4} The condition is characterized by normal development for the first 6 to 18 months of age, followed by a regression period in which individuals typically develop neurological and physical symptoms such as gait abnormalities, deceleration of head growth, loss of acquired speech, stereotypical hand movements (clapping), diminished eye contact, and breathing disturbances.^{3,5}



Although MeCP2 is expressed throughout the body, it is more abundant in brain.⁶ Correspondingly, brain-specific deletion of the *Mecp2* gene at embryonic day 12 results in a similar phenotype to that observed in a whole body knockout model, indicating that mutations in *MECP2* have a greater impact in the brain relative to other tissues.⁷ Indeed, outside of Rett syndrome, various losses in MeCP2 functionality/expression have been reported in other neuropsychiatric disorders, such as Angelman

syndrome,⁸ non-symptomatic mental retardation,⁹ and some forms of autism.^{10,11} Furthermore, MeCP2 related disorders are not limited to loss of function/expression, but also arise from gain of function/expression. In a condition referred to as *MECP2* duplication syndrome, a phenotype similar to that of Rett syndrome presents in individuals who have additional copies of the *MECP2* gene.¹² Therefore, specific regulation of MeCP2 is necessary for normal function and development of the brain.

The conventional model of MeCP2 binding with chromatin is dependent upon methylated DNA. However, recent experimental evidence suggests MeCP2 can bind both methylated and unmethylated genomic sequences.^{13,14} We have previously shown that MeCP2 binding at unmethylated CpG sites of the mouse *Slc6a2* promoter is functionally associated with transcriptional suppression.¹⁵ Beyond CpG, further studies have revealed that MeCP2 can bind methylated cytosine followed by adenine, cytosine, or thymine, while methylated cytosine followed by adenine has been shown to recruit MeCP2 to long genes (>100 kb), repressing transcription.^{16,17} The modified DNA nucleotide 5-hydroxymethylcytosine was also recently shown to be involved in recruitment of MeCP2 to chromatin.^{18,19} Beyond DNA enrichment, RNA immunoprecipitation combined with sequencing (RIP-seq) using anti-MeCP2 antibody shows that MeCP2 binds with several regulatory long noncoding RNAs (ncRNAs), including MALAT1 and RNCR3.²⁰ Interactions with regulatory ncRNAs represent an

CONTACT Assam El-Osta  sam.el-osta@monash.edu

*Current address: Molecular Cardiology Department of Medicine Karolinska University hospital, Stockholm, Sweden
Color versions of one or more of the figures in this article can be found online at www.tandfonline.com/khvi.

 Supplemental data for this article can be accessed at  <http://dx.doi.org/10.1080/15592294.2017.1391429>

attractive mechanism that may denote specific MeCP2-RNA dependent targeting of gene regulation.

MeCP2 is a multifunctional protein implicated in alternative splicing and microRNA processing.^{21–23} Part of this activity occurs via interactions with the spliceosome component Y box-binding protein 1 (YB1) in an RNA-dependent manner.²¹ More recently, MeCP2 was shown to bind the nuclear micro-processing subunit DGCR8 in order to suppress microRNAs targeting genes critical for neuronal development such as *CREB*, *LIMK1*, and *PUM2*.²³ Other studies have also shown physical binding of RNAs with MeCP2.^{20,24} In the context of these studies, it was anticipated that identification of MeCP2-associated small RNAs would further support the hypothesis of RNA dependent binding of MeCP2 to chromatin.

Here, we identify MeCP2-bound small RNAs using a native chromatin RIP-seq strategy in mouse primary cortical neurons and examine MeCP2 interaction with chromosomal microRNAs in regulation of chromatin binding and gene regulation.

Methods

Mouse primary cortical cell culture

Embryos of day 15 from C57BL/6 mice were used to prepare primary cortical neurons as described previously.²⁵ Isolated cortical neurons were seeded at a density of 2×10^7 cells onto poly-D-lysine treated T75 flasks and maintained in a humidified 37°C incubator with 5% CO₂. Cells were maintained in plating medium for 2 h before replacing medium with serum-free growth media consisting of neurobasal media containing B27 supplements, gentamicin and glutamine. Cultures were allowed to mature for 6 days *in vitro* (DIV) before harvesting for experiments.

RNA immunoprecipitation and massive parallel sequencing (RIP-seq)

Preparation of soluble chromatin fractions using micrococcal nuclease (MNase) digestion. Briefly, the 6 DIV primary cortical neurons were scraped off the bottom of the flask in 1 mM EDTA in PBS^{-/-} (Ca²⁺ and Mg²⁺ free) and centrifuged to pellet. Cell pellet was re-suspended and incubated in 600 μ L nucleus isolation buffer [15 mM Tris-HCl pH 7.5, 60 mM KCl, 0.5 M sucrose, 0.25 mM EDTA, 0.125 mM EGTA, 1 mM DTT, 0.5 mM PMSF, 0.15 mM spermidine, 0.15 mM spermine, 0.2% NP-40, 1 \times complete proteinase inhibitor (PI) (Roche)] for 5 min at 4°C with rotation then centrifuged for 3 min at 5000 g. The precipitate, containing cell nuclei and the supernatant, containing cytosolic fraction were recovered. The precipitate was re-suspended in 400 μ L of MNase digestion buffer [20 mM Tris-HCl, 70 mM NaCl, 20 mM KCl, 5 mM MgCl, 3 mM CaCl, 0.5 mM PMSF, 1 \times complete PI (Roche)] and 250 units of micrococcal nuclease (Worthington) were added. The MNase digestion was performed for 12 min. Digestion was stopped by addition of 16 μ L MNase stop solution (125 mM EDTA, 125 mM EGTA). The digest was centrifuged (5 min, 5000 g, 4°C) and S1 chromatin fraction (first supernatant) was collected. The pellet was lysed in 400 μ L of MNase lysis buffer (2 mM EDTA with PI) for 15 min at 4°C by rotation and lysed material was centrifuged for 5 min at 5000 g at 4°C. Second supernatant S2 was recovered and the pellet (P fraction) was re-

suspended in nuclear isolation buffer with PI. MNase digestion produced two distinct chromatin fractions designated as S1 chromatin fraction (micrococcal nuclease sensitive and mononucleosomal enriched) and S2 chromatin fraction (micrococcal nuclease resistant and oligonucleosomal enriched) as described previously.²⁶ MNase digestion of chromatin and the purity of the preparation was assessed by analyzing length of DNA fragments in each chromatin fraction by gel electrophoresis.

Sodium dodecyl sulphate polyacrylamide gel electrophoresis (SDS-PAGE). Chromatin samples (20 μ L of chromatin fraction diluted with 10 μ L dH₂O) were then heated to 85°C for 4 min and a SeeBlue[®] Plus2 pre-stained molecular weight size standard were size fractionated on 4-12% gradient gels (NuPAGE[®] Bis-Tris precast gels, Invitrogen) using NuPAGE MOPS running buffer at 120 V for 2-3 h. Proteins were transferred from the gel to prewet PVDF membranes in NuPAGE transfer buffer by electrophoresis at 30 V, overnight at 4°C. PVDF membranes were incubated in blocking buffer (3% BSA in PBST (PBS containing 0.05% v/v tween 20) for 1 h at RT. Membranes were then incubated in primary antibody (diluted 1:1000 in buffer containing PBST, 3% BSA, 0.02% sodium azide) overnight at 4°C then washed 4 times in wash buffer (0.5% skim milk in PBST). The membrane was incubated with an appropriate secondary horseradish peroxidase conjugated antibody (diluted 1:20,000 in wash buffer) for 30 min at RT with agitation followed by 4-5 washes in PBST buffer. Protein expression was visualized using enhanced chemiluminescent reagent kit (Sigma-Aldrich) and detected by exposing membranes to high performance chemiluminescent film for an optimized time. Film was developed using a Kodak X-ray developer according to the manufacturer's instructions. Antibodies used were anti-Brm (Abcam, ab15597), anti-Brg1 (Abcam, ab4081), anti-Dhx9 (ThermoFisher, PA5-19542), anti-Hp1 alpha (Abcam, ab77256), anti-MeCP2 antibody (M9317, Sigma), anti-Pol II (Millipore, 05-623).

Chromatin Immunoprecipitation on MNase digested chromatin fractions. Chromatin immunoprecipitation was performed on MNase digested chromatin fractions S1 and S2 using anti-MeCP2 antibody. To avoid RNA degradation while performing RIP, RNase free tubes and RNase inhibitor RNase-OUT reagent (Invitrogen) were used. RNA was purified from immunopurified chromatin and sequenced with massive parallel sequencing for the discovery of small ncRNAs bound by MeCP2. Briefly, 1 μ g of quantified DNA in chromatin was retained as input material. To each tube, 5 μ g of chromatin diluted in ChIP dilution buffer was added, along with 20 μ L of protein A Dynabeads (Invitrogen) for pre-clearing. An additional equal number of tubes were set up in parallel containing 475 μ L ChIP dilution buffer and 20 μ L of protein A Dynabeads, with either 3 μ g of anti-MeCP2 antibody (Sigma) or Rabbit IgG (non-specific antibody). All tubes were placed at 4°C with rotation for 1 h for pre-clearing and pre-binding. Pre-cleared chromatin was separated from beads using a magnetic rack (Invitrogen) and was transferred to a parallel set of tubes containing beads pre-bound to antibodies. RNaseOUT reagent was added to the tubes and incubated overnight at 4°C with rotation in order to precipitate chromatin. The next day, chromatin-bound beads were washed twice consecutively with 0.5 mL of the following buffers, in order: low salt buffer, high salt buffer, LiCl buffer, and TE buffer. RNaseOUT was added

to all wash buffers. After washes, CHIP elution buffer was added to the retained input material and to antibody and no-antibody or IgG controls and sample pooled together into anti-MeCP2 antibody bound, No antibody or IgG-bound control, and Input. RNA was purified using Trizol and mirVana miRNAs isolation kit (Ambion).

Deep sequencing of the immunopurified small ncRNAs. We performed deep sequencing of the immunopurified small ncRNAs from active and silent chromatin. Small RNAs were converted into cDNA and sequenced using the Illumina high-throughput sequencing. A cDNA library was prepared according to the Illumina Small RNA v1.5 protocol. Briefly, adapters were ligated at 3' and 5' ends of the RNA and RNA was then reverse transcribed to cDNA, after which cDNA was amplified for 14 or 18 cycles of PCR. Complimentary DNA libraries were size-selected on an agarose gel. The quality and quantity of the library was evaluated using the Shimadzu MultiNA. Sequencing was performed for 51 cycles using the Genome Analyzer IIX, according to the manufacturer's protocols. Image analysis and base calling were performed using the software supplied with the Genome Analyzer instrument.

Bioinformatics analysis of RIP-seq data

Alignment of the sequenced reads to the mouse genome (GRCm38/mm10) was performed using OLEGO spliced read alignment program.²⁷ A matrix file was generated using read counts for all gene transcripts from each sample derived from the bam files. In the matrix, transcript IDs were placed in rows and sample names were placed in columns. Paired analysis was performed using the Bioconductor package edgeR²⁸ to detect RNA transcripts bound by MeCP2. Transcripts enriched from each fraction was normalized to their respective input (Total RNA isolated from S1 and S2 chromatin fraction). A paired factorial statistical analysis method was used to detect transcripts with increased enrichment in the S2 chromatin fraction relative to S1. RNA transcripts were considered significantly enriched, if the Benjamini-Hochberg false discovery rate (FDR) adjusted *P* value was less than 0.05.

Quantitative RT-PCR to validate RIP-seq

RIP-seq data was validated by qRT-PCR using miScript RT PCR II kit (Qiagen) and miScript microRNA primer assays following manufacturer's instructions. Interaction of miRNAs with MeCP2 in the soluble S1 and S2 fractions was determined by comparing % input of anti-MeCP2 bound normalized to the % input of the no antibody control. Data is presented as percent input corrected for no antibody control samples. For RNase digestion, immunopurified RNA was digested with RNase A solution (Sigma, R4642) at a final concentration of 10 μ g/ml and incubated at RT for 10 min prior to RNA purification.

RIP PCR in mouse cerebellum

Nuclei obtained from mouse cerebellum were digested with MNase to prepare S1 and S2 chromatin fractions. RIP using anti-MeCP2 antibody was performed in both chromatin fractions. RNA was isolated from immunoprecipitated chromatin

using Trizol and RNeasy MinElute kit (Qiagen). Complementary DNA synthesis and qRT-PCR were performed with miScript microRNA RT PCR kit from Qiagen. Binding of microRNAs with MeCP2 was determined by comparing percent input of anti-MeCP2 with the percent of input of non-specific IgG antibody.

MeCP2 mouse model

Mecp2 wild type (129/C57BL6 background) and symptomatic *Mecp2* Null (*Mecp2tm1Tam*) were used for RNA sequencing. *Mecp2* Null mice became symptomatic at ages between 8-14 weeks based on the phenotypic development of body trembling, labored breathing, and hind-limb clasping. Therefore, RNA isolated from these mice were used for RNA sequencing.

RNA-seq

Total RNA was extracted from the cerebellum of *Mecp2* wild type (129/C57BL6 background) and symptomatic *Mecp2* Null (*Mecp2tm1Tam*) male mice aged 8-14 weeks using TRIzol reagent. Equal amounts of total RNA (5 μ g per sample) were subsequently used in the construction of sequencing libraries using a RNA-sequencing library preparation kit (Illumina). Sequencing of the RNA-seq libraries was performed with a Genome Analyzer IIX (Illumina), and a 36-cycle version 4 sequencing kit (Illumina) according to the manufacturer's protocol. Sequence and quality data were extracted from cluster cycle imaging using Pipeline v1.6 software (Illumina) and aligned to the mouse genome (July 2007 NCBI37/mm9 assembly) using the burrows-wheeler aligner.²⁹ Aligned reads were imported into the SeqMonk software package in which reads were quantified for overlapping gene transcripts. Transcript read counts were normalized for total sample reads before relative quantitation between samples. Heatmaps were generated using the R package, ComplexHeatmaps.³⁰ One of the *Mecp2* Null samples was excluded because of abnormal 3 prime distribution of sequencing reads. The remaining *Mecp2* Null sequencing data was compared with each WT set to screen for changes in expression overall. However, we believe that the data reflects the generalized pattern of changes in *Mecp2* Null models and this is consistent with previous studies that indicate suppression of gene expression by MeCP2. At least two other studies have presented CHIP—microarray data that show a majority of genes have a lower expression in the absence of MeCP2 in both *in vitro* and *in vivo* settings.^{13,14}

Analysis of gene targets of MeCP2 interacting microRNAs

Genes were ranked by significance and fold change as described previously³¹ prior to Gene Set Enrichment Analysis (GSEA).³² Reactome pathway gene sets were obtained from MSigDB version 5.2 (<http://software.broadinstitute.org/gsea/msigdb>).³³ In addition, gene targets of microRNA were obtained from the starBase mouse microRNA database (2016 release)³⁴ and converted into GMT format for GSEA to determine if microRNA gene targets are generally suppressed or activated in *Mecp2* null mice. GSEA was run using the classical scoring method with 1000 permutations.

Results

RNA immunoprecipitation combined with sequencing (RIP-seq) identified MeCP2 interacting microRNAs

Since native RNA immunoprecipitation (nRIP) was the method of choice to identify MeCP2 interacting chromosomal RNAs, nuclei from mouse primary cortical neurons were subjected to MNase digestion to prepare soluble chromatin for nRIP (Fig. 1A). DNA gel electrophoresis showed that MNase digestion of nuclei isolated from mouse primary cortical neurons

generated distinct chromatin fractions (Fig. 1B). Western blot analysis of chromatin fractions was performed using antibodies against MeCP2, HP1 α , Pol II, and other protein components of MeCP2 co-regulatory complex such as Brg1, Brm, and Dhx9. In the mouse primary cortical neurons, MeCP2 was detected in both S1 and S2 chromatin fractions (Fig. 1C). Thus, we performed nRIP in both chromatin fractions. RNA was isolated from immunopurified complexes captured with anti-MeCP2 antibody. Purified RNA was sequenced with massive parallel sequencing platform to discover chromosomal RNAs bound by

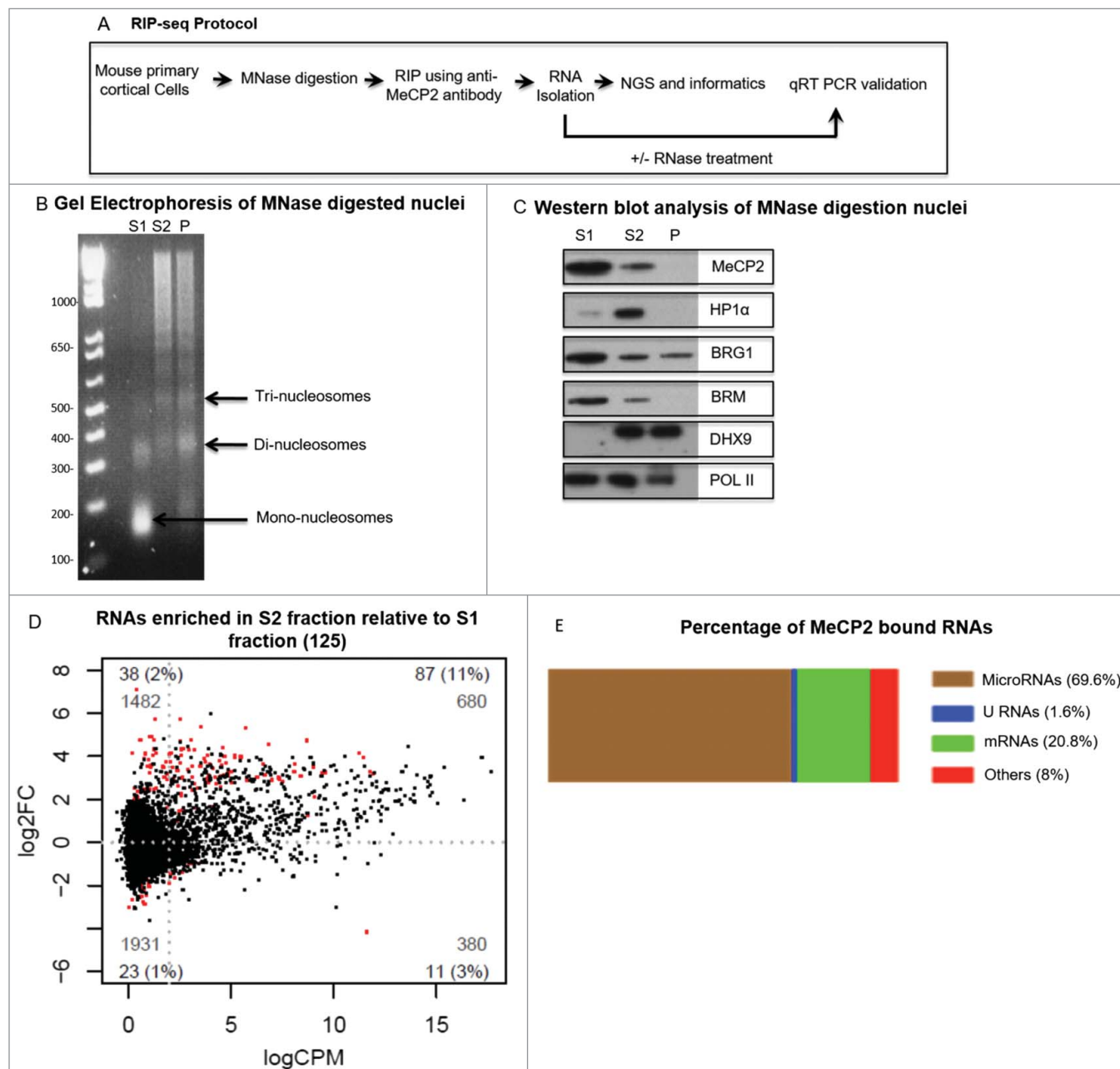


Figure 1. RNA immunoprecipitation sequencing (RIP-seq) analysis. (A) Illustration of native RNA immunoprecipitation combined with massive parallel sequencing (nRIP-seq) protocol. (B-C) Micrococcal nuclease digestion of mouse primary cortical neurons. (B) Gel electrophoresis of DNA purified from different fractions in mouse primary cortical neurons after MNase digestion for 12 minutes. S1 is MNase sensitive chromatin fraction contains mainly mononucleosomes whereas S2 is MNase resistant chromatin fraction containing nucleosomal ladder (Di, Tri and so on). (C) Western blot analysis of MNase digested chromatin fractions in mice cortical neurons with antibodies against MeCP2, Hp1 α , Brg1, Brm, Dhx9, and Pol II. (D) Smear plots showing log₂ fold change (log₂FC) plotted against log₂ counts per million (CPM). Red dots on positive scale in plot represent small transcripts (125) with increased binding with MeCP2 in MNase resistant S2 chromatin fraction relative to MNase sensitive S1 chromatin fraction. (E) Percentage of different classes of RNA transcripts bound with MeCP2 where microRNAs were the most abundant small ncRNAs that were bound by MeCP2.

MeCP2. Total chromatin bound RNA termed as input was also sequenced to normalized immunopurified RNAs. Screening of MeCP2 immunopurified complexes identified several RNAs including protein coding and noncoding RNAs such as microRNAs. Paired factorial analysis of deep sequencing data identified enrichment of 125 transcripts by MeCP2 in S2 chromatin fraction relative to MNase sensitive S1 chromatin fraction as shown by red dots in Fig. 1D. Of 125 transcripts, 87 were microRNAs that was the most abundant class of MeCP2-bound small RNA transcripts (69.6%) (Fig. 1E). Individual microRNAs and fold enrichment is presented in Table 1. Supplemental Table 1 represents transcripts other than microRNAs identified by RIP-seq.

Validation of RIP-seq data by qRT PCR

In order to verify that the candidate MeCP2 binding small RNAs identified with deep sequencing represent true interaction and not artifacts from sequencing or bioinformatics processing, PCR validation was undertaken. RNA-MeCP2 interactions in mouse primary cortical neurons were investigated using microRNA specific qPCR assays. Enrichment of microRNA by RIP-PCR is expressed as % input bound by MeCP2 normalized to % input bound by no antibody (beads only). The binding of 5 microRNAs including miR-375, miR-126, miR-455, miR-542, and *let-7i* was determined in S1 and S2 chromatin fractions. Binding of these microRNAs with MeCP2 was significantly increased in S2 chromatin fraction relative to S1 chromatin fraction, which was consistent with the RIP-seq data (Fig. 2A). Optimization experiments for the RIP protocol using RNase confirm qRT-PCR amplification signal is derived from RNA and not DNA. The immunopurified RNA was digested with RNase A enzyme before cDNA synthesis. RNase treatment significantly reduced amplification of MeCP2 interacting microRNAs miR-375, miR-126, and *let-7i* from both S1 and S2 chromatin fractions (Fig. 2B-D).

MeCP2 binds microRNAs in vivo in mouse cerebellum

MeCP2-RIP was performed in MNase digested chromatin fractions from mouse cerebellum to show that MeCP2 also binds microRNAs *in vivo*. RIP followed by microRNA specific qRT-PCR for microRNAs miR-375, miR-126, and *let-7i* showed MeCP2 interaction with these microRNAs. MicroRNAs miR-375, miR-126, and *let-7i* were significantly enriched with MeCP2 in S2 chromatin fraction in mice cerebellum. These results confirm MeCP2 binds microRNAs *in vivo* in mouse cerebellum presented in Fig. 3A-B.

Gene expression changes in MeCP2 null mouse cerebellum and gene targets of MeCP2-interacting microRNAs

MeCP2 is a nuclear protein with increased affinity to bind methylated DNA. Global gene expression has been measured previously in Rett mouse model.³⁵ We sequenced mRNA specifically to identify targets of MeCP2 protein in mice cerebellum. Fig. 4A represents a heat map showing top 50 genes dysregulated in mouse cerebellum when *Mecp2* was knocked out. Reactome Gene Set Enrichment Analysis (GSEA) revealed

Table 1. List of microRNAs with increased binding to MeCP2 in the MNase resistant S2 chromatin fraction relative to the S1 chromatin fraction and discovered with small RIP-seq. Chromatin fractions were isolated from mouse primary cortical neurons. FC, Fold change; CPM, count per million; adjusted *P* value, FDR. Samples ordered in sequence of highest to lowest *P* value.

Name	logFC S2 relative to S1	logCPM S2 relative to S1	Adjusted <i>P</i> value S2 relative to S1
ENSMUSG00000065616_Mir375	5.7236	1.2889	9.3219E-16
ENSMUSG00000065445_Mir143	5.3202	5.7183	1.6413E-12
ENSMUSG00000065601_Mir146	4.3887	4.5887	1.4796E-09
ENSMUSG00000065529_Mir22	4.0697	5.1515	1.0101E-07
ENSMUSG00000065526_Mir337	3.5443	3.1029	1.9034E-07
ENSMUSG00000085148_Mir22hg	3.9599	5.1649	1.9394E-06
ENSMUSG00000065444_Mir27a	3.8220	0.9588	2.6029E-06
ENSMUSG00000065540_Mir126	5.3568	3.5255	2.1864E-05
ENSMUSG00000077921_Mir872	3.0591	4.8706	2.4842E-05
ENSMUSG00000065603_Mir218-1	4.7393	0.5784	2.4842E-05
ENSMUSG00000093337_Mir5109	2.1246	9.0693	4.4918E-05
ENSMUSG00000070102_Mir455	4.1022	1.9968	7.2821E-05
ENSMUSG00000093026_mmu-mir-378a	4.0000	4.6699	1.4986E-04
ENSMUSG00000076361_Mir182	4.7561	3.0580	2.1953E-04
ENSMUSG00000065565_Mir181a-1	3.9722	5.4701	2.2832E-04
ENSMUSG00000070110_Mir504	4.9274	1.1584	2.3487E-04
ENSMUSG00000065490_Mir30c-1	3.5235	0.9244	2.3487E-04
ENSMUSG00000065515_Mir152	3.7306	3.7416	2.5227E-04
ENSMUSG00000089357_Mir2137	4.3250	1.2561	3.1367E-04
ENSMUSG00000093291_mmu-mir-299b	3.9091	0.7569	3.2010E-04
ENSMUSG00000076052_Mir541	3.2833	8.0734	3.2535E-04
ENSMUSG00000065479_Mir125a	2.9606	7.3353	4.0182E-04
ENSMUSG00000065619_Mir183	4.3280	2.5586	4.7651E-04
ENSMUSG00000092984_Mir5115	3.2621	4.9969	6.4777E-04
ENSMUSG00000065493_Mir34a	4.9099	1.0441	7.8736E-04
ENSMUSG00000070109_Mir497	4.9292	1.0330	1.1072E-03
ENSMUSG00000065574_Mir203	3.0769	4.4668	1.1278E-03
ENSMUSG00000093108_Mir344f	4.7679	1.2487	1.4456E-03
ENSMUSG00000092876_mmu-mir-9-1	3.2319	1.0412	1.8314E-03
ENSMUSG00000065505_Mir148a	4.7333	8.6709	1.8516E-03
ENSMUSG00000070129_Mir136	3.0353	4.2290	1.8866E-03
ENSMUSG00000065589_Mir301	2.9921	2.2141	1.8969E-03
ENSMUSG00000065530_Mir99a	3.9546	11.4561	2.3855E-03
ENSMUSG00000065590_Mir212	3.3449	2.3841	2.4216E-03
ENSMUSG00000065583_Mir218-2	3.6369	3.9330	2.4216E-03
ENSMUSG00000093224_mmu-mir-380	4.0628	3.8551	2.5789E-03
ENSMUSG00000065434_Mir7-1	2.5356	3.3770	3.0706E-03
ENSMUSG00000070076_Mir127	3.5064	8.9905	3.5340E-03
ENSMUSG00000065429_Mir345	3.4412	4.1212	3.9509E-03
ENSMUSG00000065532_Mir187	3.0074	2.6240	5.2249E-03
ENSMUSG00000093046_Mir3081	3.5110	1.6448	5.3507E-03
ENSMUSG00000092995_Mir16-1	2.6095	2.4160	5.3507E-03
ENSMUSG00000065607_Mir331	3.6915	2.5022	5.3814E-03
ENSMUSG00000088148_Mir1983	3.3683	2.8936	8.2724E-03
ENSMUSG00000065538_Mir153	2.4791	0.8858	9.6861E-03
ENSMUSG00000080331_Mir1298	4.5784	6.8219	1.0597E-02
ENSMUSG00000065494_Mir28	3.9165	3.6876	1.1353E-02
ENSMUSG00000065579_Mir425	4.7262	2.5114	1.1776E-02
ENSMUSG00000065415_Mir217	4.1240	0.8310	1.2468E-02
ENSMUSG00000092915_mmu-mir-191	3.0043	7.3223	1.2571E-02
ENSMUSG00000065472_Mir125b-2	3.1532	4.8656	1.3091E-02
ENSMUSG00000065409_Mir30e	2.9034	6.9804	1.3867E-02
ENSMUSG00000070101_Mir341	3.5452	3.5018	1.4092E-02
ENSMUSG00000065483_Mir181c	3.1394	4.6644	1.4272E-02
ENSMUSG00000070074_Mir484	2.7291	4.2684	1.4808E-02
ENSMUSG00000065410_Mir298	3.0132	6.2660	1.5344E-02
ENSMUSG00000065433_Mir370	3.6509	8.0840	1.5386E-02
ENSMUSG00000065406_Mirlet7i	3.1816	11.9423	1.7820E-02
ENSMUSG00000076338_Mir181d	3.0143	7.8515	1.8980E-02
ENSMUSG00000065609_Mir7-2	4.1393	1.3322	1.9095E-02
ENSMUSG00000065560_Mir148b	3.6616	6.5430	2.5005E-02
ENSMUSG00000093238_Mir9-3	4.3474	2.6964	2.7670E-02
ENSMUSG00000065567_Mir30c-2	3.7779	4.4308	2.8376E-02
ENSMUSG00000065423_Mir181a-2	3.5691	4.5353	2.8376E-02
ENSMUSG00000089726_Mir17hg	3.2364	9.4175	2.8471E-02
ENSMUSG00000065426_Mir134	3.6948	4.7557	3.2208E-02
ENSMUSG00000065428_Mir382	3.1401	6.6342	3.4257E-02

(continued)

Table 1. (Continued)

Name	logFC S2 relative to S1	logCPM S2 relative to S1	Adjusted P value S2 relative to S1
ENSMUSG00000065577_Mir329	4.0540	2.5779	3.4371E-02
ENSMUSG00000093011_Mir100	4.1421	11.2520	3.4925E-02
ENSMUSG00000072900_Mir540	3.5130	1.0657	3.4925E-02
ENSMUSG00000070080_Mir431	3.1441	3.8900	3.6217E-02
ENSMUSG00000070100_Mir362	2.7667	2.1171	3.6707E-02
ENSMUSG00000065570_Mir412	3.5721	1.1110	3.7874E-02
ENSMUSG00000076140_Mir542	3.5096	2.1533	4.2872E-02
ENSMUSG00000065536_Mir98	2.7844	5.0088	4.3073E-02
ENSMUSG00000080441_Mir1249	2.4492	1.0397	4.4226E-02
ENSMUSG00000070139_Mir532	2.8454	7.5266	4.6602E-02
ENSMUSG00000070130_Mir328	3.2948	4.8399	4.6602E-02
ENSMUSG00000065613_Mir92-2	4.1678	2.0651	4.6602E-02
ENSMUSG00000065551_Mir210	3.0160	3.1104	4.6602E-02
ENSMUSG00000065542_Mir224	3.7459	1.8243	4.6602E-02
ENSMUSG00000065524_Mir135a-2	3.1806	1.8864	4.6602E-02
ENSMUSG00000065450_Mir448	3.7226	2.0543	4.6602E-02
ENSMUSG00000065431_Mir186	2.5933	4.4717	4.6602E-02
ENSMUSG00000080669_Mir1224	3.5073	1.7346	4.8296E-02
ENSMUSG00000092988_Mir3093	2.4630	1.2308	4.8368E-02
ENSMUSG00000065471_Mir222	4.3033	3.1861	4.8368E-02

dysregulation of pathways with neurological significance including the inhibition of ligand gated ion channels and GABA A receptor activation, as well as induction of pathways related to carbohydrate metabolism and L1CAM interactions (Fig. 4B).

If MeCP2 is required for the nuclear action of microRNAs, then the target genes of these microRNAs will likely be dysregulated in *Mecp2* null mouse. To determine whether miRNA target gene sets are collectively altered in expression, we curated a database of empirically determined target genes of 303 mature microRNAs³⁴ and evaluated their differential expression using GSEA. From the 303 microRNA target sets, 296 sets contained 10 or more genes detected in the *Mecp2* null mouse. Of these, 206 sets demonstrated a significant ($FDR \leq 0.05$) inhibition of expression, while none showed a statistically significant increase (Fig. 4C). Of the 87 MeCP2 interacting microRNAs, there were 57 with target gene sets included in this enrichment analysis and all showed statistically significant inhibition of target genes (Fig. 4D). These results support the notion that MeCP2 binding at these loci may be associated with its interaction with microRNAs.

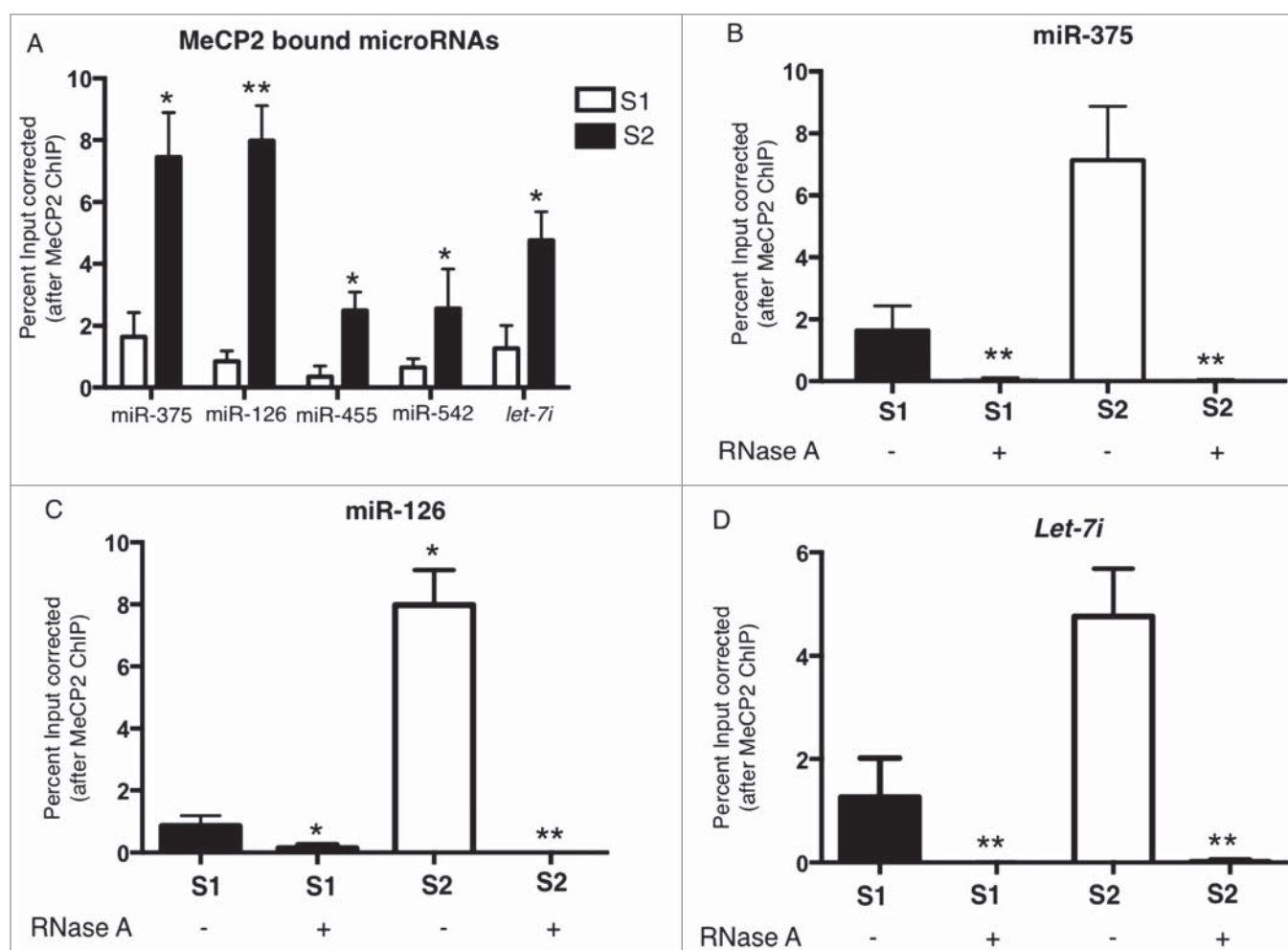


Figure 2. Validation of RIP-seq data using qRT-PCR. MeCP2-RNA candidate interactions were validated in mouse primary cortical neurons using qRT PCR. (A) Data presented as percent of input (total chromatin RNA) bound by MeCP2 and normalized to the percent input bound in no antibody control samples. (B) MicroRNA miR-375 qRT PCR with and without RNase treatment. (C) MicroRNA miR-126 qRT PCR after RNase A treatment of MeCP2 bound RNAs in mouse primary cortical neurons. RNase A treatment of RNA isolated after MeCP2-RIP decreased amplification of miR-126 from both S1 and S2 chromatin fractions. (D) *Let-7i* qRT PCR after RNase A treatment of MeCP2 bound RNAs in mouse primary cortical neurons. RNase A treatment of RNA isolated after MeCP2-RIP decreased amplification of *let-7i* from both S1 and S2 chromatin fractions; S1, MNase sensitive chromatin fraction; S2, MNase resistant chromatin fraction; n = 3; t test * $P < 0.05$, ** $P < 0.01$; error bars represent mean \pm SEM.

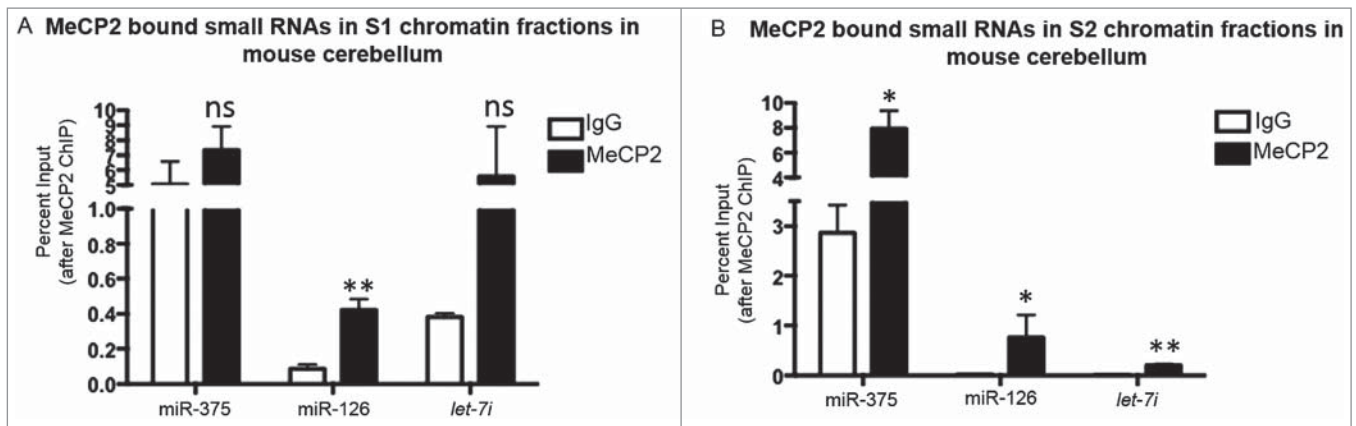


Figure 3. MeCP2 interaction with chromosomal RNA in mouse cerebellum. Candidate MeCP2-RNA interactions were also validated *in vivo* in mouse cerebellum using qRT PCR (A) MeCP2 and candidate microRNAs interactions in S1 chromatin fraction. (B) MeCP2 and candidate microRNAs interactions in S2 chromatin fraction; n = 3; Paired t test * $P < 0.05$, ** $P < 0.01$; error bars represent mean \pm SEM.

Discussion

Growing evidence suggests that DNA methylation is not necessary for MeCP2 chromatin binding.^{15,36} RIP combined with sequencing identified small RNAs including microRNAs bound by MeCP2 in mouse primary cortical neurons. Targets of these microRNAs include several genes that are dysregulated in *Mecp2* null mice cerebellum. This suggests that MeCP2 binding may be regulated in an RNA dependent manner to regulate gene expression. We have previously identified several long ncRNAs including MALAT1 and RNCR3 associated with MeCP2 by RIP-seq with formaldehyde cross linking and sequencing libraries without size selection.²⁰ Here, native RIP combined with small RNA sequencing was performed using mouse primary cortical neurons. Performing nRIP with increased antibody specificity and efficiency and small RNA sequencing enhances confidence in identifying novel interaction of small RNAs with MeCP2.

Our current findings suggest that the MeCP2 interactions might also be regulated in an RNA-dependent manner. Non-coding RNAs have been implicated in transcriptional gene regulation.³⁷ The best-characterized lincRNAs, XIST and HOTAIR, have been shown to repress transcription by recruiting the chromatin modifying enzyme complexes such as PRC2.^{38–40} Previous experimental evidence suggests that conserved components of the RNAi machinery direct the formation of chromatin assembly by sequence-specific siRNA.⁴¹ Although a mechanism by which ncRNAs could regulate MeCP2 binding to chromatin remains to be determined, ncRNAs are speculated to guide MeCP2 to chromatin to regulate gene expression.

The majority of MeCP2 bound small RNA transcripts in our RIP-seq data were microRNAs (69.6%). They are short non-coding RNAs that regulate gene expression. Previous experimental identification of the majority of nuclear identified small RNAs belong to microRNAs class of ncRNA, which supports the abundance of microRNA in our small RIP-seq data.^{42,43} In the present study, we identified a novel MeCP2 interaction with chromosomal microRNAs and hypothesize putative roles in transcriptional regulation. While MeCP2 is known to bind

to chromatin in the context of methylated DNA, the experimental results described here suggest an expansion of roles that include transcriptional regulation mediated by interacting microRNAs. Becoming an integral component of our view of the transcriptional mechanisms of gene expression, miRNAs are emerging as regulatory nodes coordinated by signaling molecules. For example, MeCP2 suppresses miR-195 processing by regulating the DGCR8/Drosha complex that play critical roles in neural development.²³ MeCP2 interferes with the assembly of Drosha and DGCR8 complex, which is implicated in targets of MeCP2-suppressed microRNAs such as CREB. Phosphorylation of MeCP2 regulates an intramolecular switch for binding to DGCR8 and suggest the control of microRNA processing represents a mechanism of gene regulation and neural development. Recently, using a novel assay—RNA of isolated chromatin combined with deep sequencing (RICH-seq)—we have identified microRNA *Let-7i* mediated *NET* gene suppression by MeCP2 in Postural tachycardia syndrome.⁴⁴ Because miRNA processing is a highly-regulated process it is not surprising to reveal that almost half of the MeCP2 bound microRNAs are altered in expression from KO mice show³⁵ and consistent with our experimental observations derived from RIP-seq. While this large dataset requires functional validation, our computational analysis supports the notion that the microRNAs may influence the capacity of MeCP2 to interact with chromatin to regulate gene expression.

MeCP2 interaction with microRNAs was also evident *in vivo* in mouse cerebellum. Results of RIP followed by qRT PCR in mouse cerebellum provided further support for MeCP2 interaction with microRNAs highlighting the potential importance for these interactions in the brain *in vivo*.

Our novel findings presented here suggest a new mechanism of RNA dependent MeCP2 binding on chromatin. Interaction of chromosomal microRNAs with MeCP2 represents an additional complexity in its genome-wide binding. While the experimental data presented here suggest MeCP2 is a prime candidate for microRNA mediated regulation, we cannot rule out regulatory components of the MeCP2 complex influence context-dependent microRNA binding. The limitation of the study is that starbase predicted targets of MeCP2 interacting

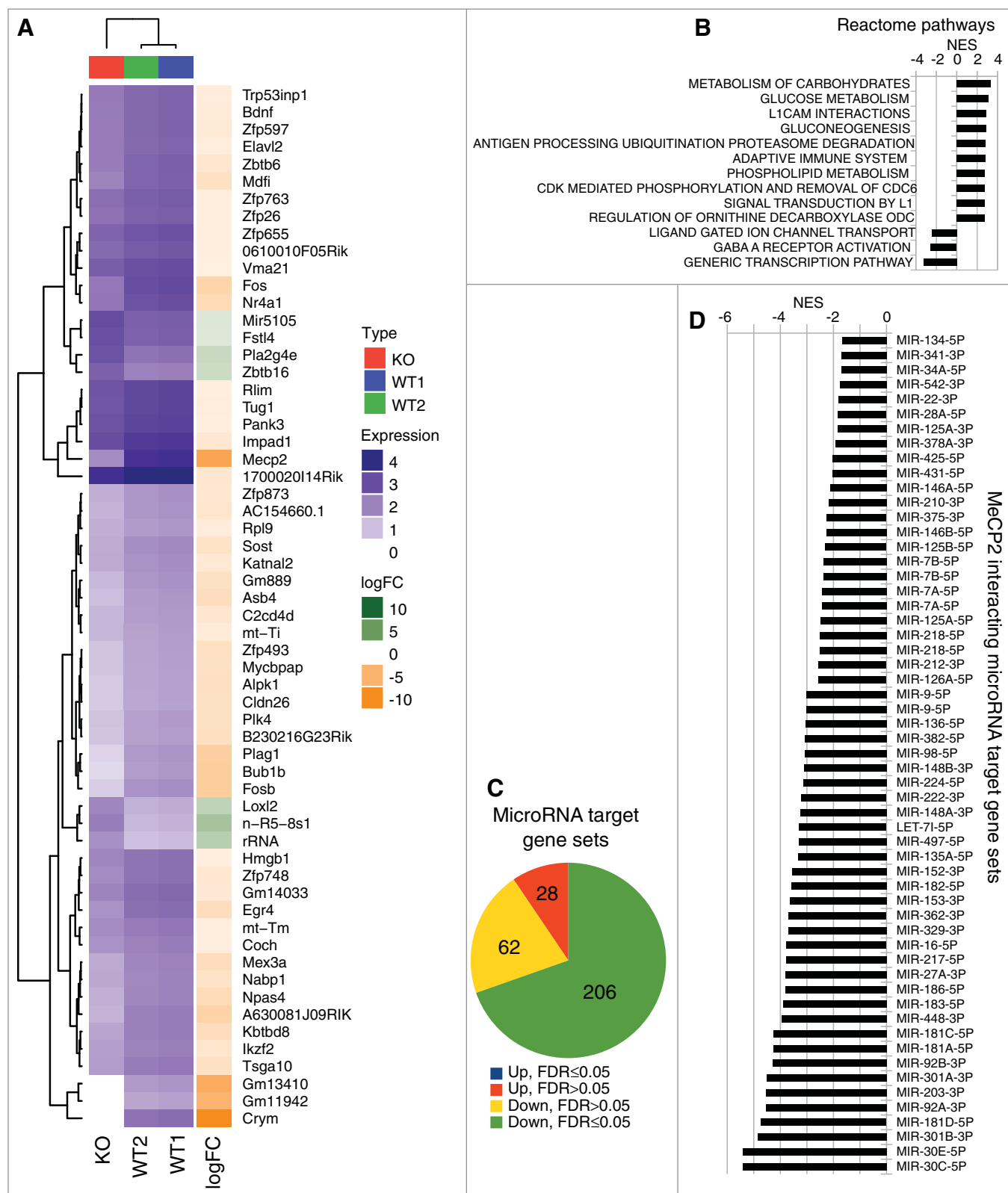


Figure 4. Gene sets targeted by MeCP2 interacting microRNAs. (A) Gene expression changes in *Mecp2* null mouse cerebellum. Heat map showing a list of top 50 genes dysregulated in *Mecp2* null mouse cerebellum compared to wild type mouse cerebellum. The top 50 genes were determined by the absolute fold change. (B) Reactome pathway analysis using GSEA. Up to 10 statistically significant ($FDR \leq 0.05$) gene sets in the up- and down-regulated direction. (C) Summary of GSEA using microRNA target genes from Starbase. Of the 296 sets of microRNA target genes, 206 are significantly downregulated ($FDR \leq 0.05$, green color). (D) MeCP2-interacting microRNA target gene sets are all inhibited ($FDR \leq 0.05$) in *Mecp2* null mouse model.

microRNAs need to be experimentally validated. These results support the involvement of microRNAs in mediating MeCP2 associated gene regulation in the brain. Future studies are required to understand the importance of MeCP2 interaction with microRNAs.

Data availability

Deep sequencing data is available from the GEO database under accession GSE107085.

Acknowledgements

The *Mecp2* Null mouse model tissues were kindly provided by Gregory Pelka and Patrick Tam

Funding

This study was supported by a National Health and Medical Research Council (NHMRC) program grants (Numbers APP0526681, APP1113188). We acknowledge the fellowship support from the NHMRC. This work was supported in part by the Victorian Government's Operational Infrastructure Support Program.

Conflict of interest

The authors have declared that no conflict of interest exists

Author contributions

AK and AE designed the study. *AK* performed RIP-seq, validation of RIP-seq and RIP-qRT-PCR. *AK* and *GC* cultured primary cortical cells. *SM* performed RNA-seq and analyzed RNA-seq data. *MZ* performed deep sequencing. *AK*, *MZ* and *HR* analyzed RIP sequencing data. *MZ* and *HR* performed analysis to identify gene targets of MeCP2 interacting microRNAs. *AK*, *MZ* and *HR* prepared figures. *AK*, *SM* and *AE* co-wrote the manuscript, which has been edited by *HR*, *GC*, and *MZ*. All authors have read and approved the submitted manuscript.

References

- Lewis JD, Meehan RR, Henzel WJ, Maurer-Fogy I, Jeppesen P, Klein F, Bird A. Purification, sequence, and cellular localization of a novel chromosomal protein that binds to methylated DNA. *Cell*. 1992;69(6):905–14. doi:10.1016/0092-8674(92)90610-O.
- Amir RE, Van den Veyver IB, Wan M, Tran CQ, Francke U, Zoghbi HY. Rett syndrome is caused by mutations in X-linked MECP2, encoding methyl-CpG-binding protein 2. *Nat genetics*. 1999;23(2):185–8. doi:10.1038/13810.
- Hagberg B, Aicardi J, Dias K, Ramos O. A progressive syndrome of autism, dementia, ataxia, and loss of purposeful hand use in girls: Rett's syndrome: report of 35 cases. *Ann Neurol*. 1983;14(4):471–9. doi:10.1002/ana.410140412.
- Rett A. [The care of mentally defective children]. *Krankenschwester*. 1966;19(3):33–5.
- Armstrong DD. Rett syndrome neuropathology review 2000. *Brain Dev*. 2001;23(Suppl 1):S72–6. doi:10.1016/S0387-7604(01)00332-1.
- Jung BP, Jugloff DG, Zhang G, Logan R, Brown S, Eubanks JH. The expression of methyl CpG binding factor MeCP2 correlates with cellular differentiation in the developing rat brain and in cultured cells. *J Neurobiol*. 2003;55(1):86–96. doi:10.1002/neu.10201.
- Akbadian S, Chen RZ, Gribnau J, Rasmussen TP, Fong H, Jaenisch R, Jones EG. Expression pattern of the Rett syndrome gene MeCP2 in primate prefrontal cortex. *Neurobiol Dis*. 2001;8(5):784–91. doi:10.1006/nbdi.2001.0420.
- Watson P, Black G, Ramsden S, Barrow M, Super M, Kerr B, Clayton-Smith J. Angelman syndrome phenotype associated with mutations in MECP2, a gene encoding a methyl CpG binding protein. *J Med Genet*. 2001;38(4):224–8. doi:10.1136/jmg.38.4.224.
- Miltenberger-Miltenyi G, Laccione F. Mutations and polymorphisms in the human methyl CpG-binding protein MECP2. *Hum Mutat*. 2003;22(2):107–15. doi:10.1002/humu.10243.
- Samaco RC, Nagarajan RP, Braunschweig D, LaSalle JM. Multiple pathways regulate MeCP2 expression in normal brain development and exhibit defects in autism-spectrum disorders. *Hum Mol Gen*. 2004;13(6):629–39. doi:10.1093/hmg/ddh063.
- Shibayama A, Cook EH, Jr., Feng J, Glanzmann C, Yan J, Craddock N, Jones IR, Goldman D, Heston LL, Sommer SS. MECP2 structural and 3'-UTR variants in schizophrenia, autism and other psychiatric diseases: a possible association with autism. *Am J Med Genet B Neuro-psychiatr Genet*. 2004;128B(1):50–3. doi:10.1002/ajmg.b.30016.
- Van Esch H, Bauters M, Ignatius J, Jansen M, Raynaud M, Hollanders K, Lugtenberg D, Bienvenu T, Jensen LR, Gecz J, et al. Duplication of the MECP2 region is a frequent cause of severe mental retardation and progressive neurological symptoms in males. *Am J Hum Genet*. 2005;77(3):442–53. doi:10.1086/444549.
- Yasui DH, Peddada S, Bieda MC, Vallero RO, Hogart A, Nagarajan RP, Thatcher KN, Farnham PJ, LaSalle JM. Integrated epigenomic analyses of neuronal MeCP2 reveal a role for long-range interaction with active genes. *Proc Natl Acad Sci USA*. 2007;104(49):19416–21. doi:10.1073/pnas.0707442104.
- Chahrour M, Jung SY, Shaw C, Zhou X, Wong ST, Qin J, Zoghbi HY. MeCP2, a key contributor to neurological disease, activates and represses transcription. *Science*. 2008;320(5880):1224–9. doi:10.1126/science.1153252.
- Harikrishnan KN, Bayles R, Ciccotosto GD, Maxwell S, Cappai R, Pelka GJ, Tam PP, Christodoulou J, El-Osta A. Alleviating transcriptional inhibition of the norepinephrine slc6a2 transporter gene in depolarized neurons. *The Journal of neuroscience: the official journal of the Society for Neuroscience*. 2010;30(4):1494–501. doi:10.1523/JNEUROSCI.4675-09.2010.
- Guo JU, Su Y, Shin JH, Shin J, Li H, Xie B, Zhong C, Hu S, Le T, Fan G, et al. Distribution, recognition and regulation of non-CpG methylation in the adult mammalian brain. *Nat Neurosci*. 2014;17(2):215–22. doi:10.1038/nn.3607.
- Gabel HW, Kinde B, Stroud H, Gilbert CS, Harmin DA, Kastan NR, Hemberg M, Ebert DH, Greenberg ME. Disruption of DNA-methylation-dependent long gene repression in Rett syndrome. *Nature*. 2015;522(7554):89–93. doi:10.1038/nature14319.
- Mellen M, Ayata P, Dewell S, Kriaucionis S, Heintz N. MeCP2 binds to 5hmC enriched within active genes and accessible chromatin in the nervous system. *Cell*. 2012;151(7):1417–30. doi:10.1016/j.cell.2012.11.022.
- Spruijt CG, Gnerlich F, Smits AH, Pfaffeneder T, Jansen PW, Bauer C, Munzel M, Wagner M, Muller M, Khan F, et al. Dynamic readers for 5-(hydroxy)methylcytosine and its oxidized derivatives. *Cell*. 2013;152(5):1146–59. doi:10.1016/j.cell.2013.02.004.
- Maxwell SS, Pelka GJ, Tam PP, El-Osta A. Chromatin context and ncRNA highlight targets of MeCP2 in brain. *RNA Biology*. 2013;10(11):1741–57. doi:10.4161/rna.26921.
- Young JI, Hong EP, Castle JC, Crespo-Barreto J, Bowman AB, Rose MF, Kang D, Richman R, Johnson JM, Berget S, et al. Regulation of RNA splicing by the methylation-dependent transcriptional repressor methyl-CpG binding protein 2. *Proc Natl Acad Sci USA*. 2005;102(49):17551–8. doi:10.1073/pnas.0507856102.
- Maunakea AK, Chepelev I, Cui K, Zhao K. Intragenic DNA methylation modulates alternative splicing by recruiting MeCP2 to promote exon recognition. *Cell Research*. 2013;23(11):1256–69. doi:10.1038/cr.2013.110.
- Cheng TL, Wang Z, Liao Q, Zhu Y, Zhou WH, Xu W, Qiu Z. MeCP2 suppresses nuclear microRNA processing and dendritic growth by regulating the DGCR8/Drosha complex. *Developmental Cell*. 2014;28(5):547–60. doi:10.1016/j.devcel.2014.01.032.
- Jeffery L, Nakielyns S. Components of the DNA methylation system of chromatin control are RNA-binding proteins. *J Biol Chem*. 2004;279(47):49479–87. doi:10.1074/jbc.M409070200.

25. Ciccotosto GD, Tew DJ, Drew SC, Smith DG, Johanssen T, Lal V, Lau TL, Perez K, Curtain CC, Wade JD, et al. Stereospecific interactions are necessary for Alzheimer disease amyloid-beta toxicity. *Neurobiol Aging*. 2011;32(2):235–48. doi:10.1016/j.neurobiolaging.2009.02.018.
26. Okabe J, Orłowski C, Balcerzyk A, Tikellis C, Thomas MC, Cooper ME, El-Osta A. Distinguishing hyperglycemic changes by Set7 in vascular endothelial cells. *Circ Res*. 2012;110(8):1067–76. doi:10.1161/CIRCRESAHA.112.266171.
27. Wu J, Anczukow O, Krainer AR, Zhang MQ, Zhang C. OLEgo: fast and sensitive mapping of spliced mRNA-Seq reads using small seeds. *Nucleic Acids Res*. 2013;41(10):5149–63. doi:10.1093/nar/gkt216.
28. Robinson MD, McCarthy DJ, Smyth GK. edgeR: a Bioconductor package for differential expression analysis of digital gene expression data. *Bioinformatics*. 2010;26(1):139–40. doi:10.1093/bioinformatics/btp616.
29. Li H, Durbin R. Fast and accurate short read alignment with Burrows-Wheeler transform. *Bioinformatics*. 2009;25(14):1754–60. doi:10.1093/bioinformatics/btp324.
30. Gu Z, Eils R, Schlesner M. Complex heatmaps reveal patterns and correlations in multidimensional genomic data. *Bioinformatics*. 2016;32(18):2847–9. doi:10.1093/bioinformatics/btw313.
31. Rafehi H, Balcerzyk A, Lunke S, Kaspi A, Ziemann M, Kn H, Okabe J, Khurana I, Ooi J, Khan AW, et al. Vascular histone deacetylation by pharmacological HDAC inhibition. *Genome Res*. 2014;24(8):1271–84. doi:10.1101/gr.168781.113.
32. Subramanian A, Tamayo P, Mootha VK, Mukherjee S, Ebert BL, Gillette MA, Paulovich A, Pomeroy SL, Golub TR, Lander ES, et al. Gene set enrichment analysis: a knowledge-based approach for interpreting genome-wide expression profiles. *Proc Natl Acad Sci USA*. 2005;102(43):15545–50. doi:10.1073/pnas.0506580102.
33. Croft D, O’Kelly G, Wu G, Haw R, Gillespie M, Matthews L, Caudy M, Garapati P, Gopinath G, Jassal B, et al. Reactome: a database of reactions, pathways and biological processes. *Nucleic Acids Res*. 2011;39(Database issue):D691–7. doi:10.1093/nar/gkq1018.
34. Li JH, Liu S, Zhou H, Qu LH, Yang JH. starBase v2.0: decoding miRNA-ceRNA, miRNA-ncRNA and protein-RNA interaction networks from large-scale CLIP-Seq data. *Nucleic Acids Res*. 2014;42(Database issue):D92–7. doi:10.1093/nar/gkt1248.
35. Wu H, Tao J, Chen PJ, Shahab A, Ge W, Hart RP, Ruan X, Ruan Y, Sun YE. Genome-wide analysis reveals methyl-CpG-binding protein 2-dependent regulation of microRNAs in a mouse model of Rett syndrome. *Proc Natl Acad Sci USA*. 2010;107(42):18161–6. doi:10.1073/pnas.1005595107.
36. Bayles R, Harikrishnan KN, Lambert E, Baker EK, Agrotis A, Guo L, Jowett JB, Esler M, Lambert G, El-Osta A. Epigenetic modification of the norepinephrine transporter gene in postural tachycardia syndrome. *Arterioscler Thromb Vasc Biol*. 2012;32(8):1910–6. doi:10.1161/ATVBAHA.111.244343.
37. Kim DH, Saetrom P, Snove O, Jr., Rossi JJ. MicroRNA-directed transcriptional gene silencing in mammalian cells. *Proc Natl Acad Sci USA*. 2008;105(42):16230–5. doi:10.1073/pnas.0808830105.
38. Rinn JL, Kertesz M, Wang JK, Squazzo SL, Xu X, Bruggmann SA, Goodnough LH, Helms JA, Farnham PJ, Segal E, et al. Functional demarcation of active and silent chromatin domains in human HOX loci by noncoding RNAs. *Cell*. 2007;129(7):1311–23. doi:10.1016/j.cell.2007.05.022.
39. Tsai MC, Manor O, Wan Y, Mosammamaparast N, Wang JK, Lan F, Shi Y, Segal E, Chang HY. Long noncoding RNA as modular scaffold of histone modification complexes. *Science*. 2010;329(5992):689–93. doi:10.1126/science.1192002.
40. Jeon Y, Sarma K, Lee JT. New and Xisting regulatory mechanisms of X chromosome inactivation. *Curr Opin Genet Dev*. 2012;22(2):62–71. doi:10.1016/j.gde.2012.02.007.
41. Mattick JS, Amaral PP, Dinger ME, Mercer TR, Mehler MF. RNA regulation of epigenetic processes. *BioEssays: news and reviews in molecular, cellular and developmental biology*. 2009;31(1):51–9. doi:10.1002/bies.080099.
42. Khudayberdiev SA, Zampa F, Rajman M, Schrott G. A comprehensive characterization of the nuclear microRNA repertoire of post-mitotic neurons. *Front Mol Neurosci*. 2013;6:43. doi:10.3389/fnmol.2013.00043.
43. Jeffries CD, Fried HM, Perkins DO. Nuclear and cytoplasmic localization of neural stem cell microRNAs. *Rna*. 2011;17(4):675–86. doi:10.1261/rna.2006511.
44. Khan AW, Ziemann M, Corcoran SJ, K NH, Okabe J, Rafehi H, Maxwell SS, Esler MD, El-Osta A. NET silencing by let-7i in postural tachycardia syndrome. *JCI Insight*. 2017;2(6):e90183. doi:10.1172/jci.insight.90183.